Oligo(aromatic ether sulfone)-F as a Nonlinear Polarized Polymeric Material: an Experiment and DFT Study①

GAN Dong-Er[a, c] ZHANG Zhang[b, c]
LI Qiao-Hong[b] LI Wen-Mu[a②]

[a] (*Key Laboratory of Optoelectronic Materials Chemistry and Physics, Fujian Institute of Research on the Structure of Matter, Chinese Academy of Sciences, Fuzhou* 350002, *China*)

[b] (*State Key Laboratory of Structural Chemistry, Fujian Institute of Research on the Structure of Matter, Chinese Academy of Sciences, Fuzhou* 350002, *China*)

[c] (*University of Chinese Academy of Sciences, Beijing* 100049, *China*)

ABSTRACT Polymeric membranes with diverse structures have attracted much attention as new materials for nonlinear optical devices. In this report, a novel oligomer of poly (aromatic ether sulfone) (OAES) has been synthesized and characterized. The electronic structure as well as linear and nonlinear optical properties has been studied by density function theory. The effect for general nonlinear optical polarizability of various condition has been further researched such as absence of side chains and introduction of phenyl substituent on side chains. The static and frequency-dependent hyperpolarizabilities of OAES and its derivatives have been calculated. This work interprets an efficient adjustment for the frequency response and the intensity of nonlinear optical polarizability can be achieved by regulating the structure of system, which provides a new potential for the application of oligomeric materials on nonlinear optical field.

Keywords: DFT method, NLO properties, oligo(aromatic ether sulfone)-F, sum-over-states method;
DOI: 10.14102/j.cnki.0254–5861.2011–2878

1 INTRODUCTION

The development of polymeric materials with the second and third nonlinear optical properties has been the focus of optical polymer materials research for last decades[1-5]. In comparison to inorganic crystals, the organic macromolecules have considerable advantages of easier synthesis, liable modification, higher optical-damage toleration and lower cost[6-8].

Majority of reports in this field focus on the π-conjugated polymeric nonlinear optical materials, which are of a critical competence in larger hyperpolarizability and rapid response time owing to their multiple donor-acceptor systems[9-11]. The works of Muhammad Ramzan Saeed Ashraf Janjua and Miroslav Medved have studied the amplification of hyperpolarizability and electron mobility with π-spacers in polymer side chains or backbones by the analysis of density function theory. These polarized polymer materials perform well in nonlinear properties such as the second harmonic generation and all-optical matching[12, 13].

However, reports on the third-order nonlinearity of polarized non-conjugated polymers are relatively rare. The theoretical calculation of the relationship between structure and optical properties is very important for understanding the NLO properties of polymer materials[14, 15]. Some works employing the DFT to thermal degradation research of the resinic polymers made an interesting explore in this subject. Enlightened by a study under the guidance of Debesh R. Roy on the NLO analysis of poly (methyl methacrylate) (PMMA), which utilizes the DFT calculations to predict the thermal and structural properties of PMMA, another traditional plastic polymer of poly (aromatic ether sulfone) (PAES) with fluoric side chain as a remarkable grafting site can also be researched by the DFT method[16].

PAES and its derivant have always been the excellent candidate materials in the fabrication of diverse polymer

Received 15 May 2020; accepted 23 December 2020

① The authors gratefully acknowledge the financial support of the 100-Talent Program of Chinese Academy of Sciences

② Corresponding author. E-mail: liwm@fjirsm.ac.cn

membranes. In the pyramid diagram of common thermosplastic materials adapted by Peiyuan Zuo, PAES belongs to the top marked as high performance polymers for its chemical, thermal, and mechanical stability[17]. Good proton conductivity can be obtained by conveniently introducing hydrophilic structure such as sulfonic groups[18]. Owing to the great compatibility, PAES can easily form complexes with various organic and inorganic molecules, which achieved many noteworthy results in studying nanofiltration membranes and medical applications[19].

This novel PAES derived from the work of Zhao Li and Michael D. Guiver[20]. After a series of modifications on monomer like introducing massive methyl, removing the electron withdrawing group and canceling comonomer as shown in Fig. 1, the electronic cloud density and structural regularity of backbone have an obvious promotion. The consequential polymer of oligo(aromatic ether sulfone)-F provides an outstanding potential for further graft and substitution, which has many prospective applications in electrolyte membranes for fuel cells.

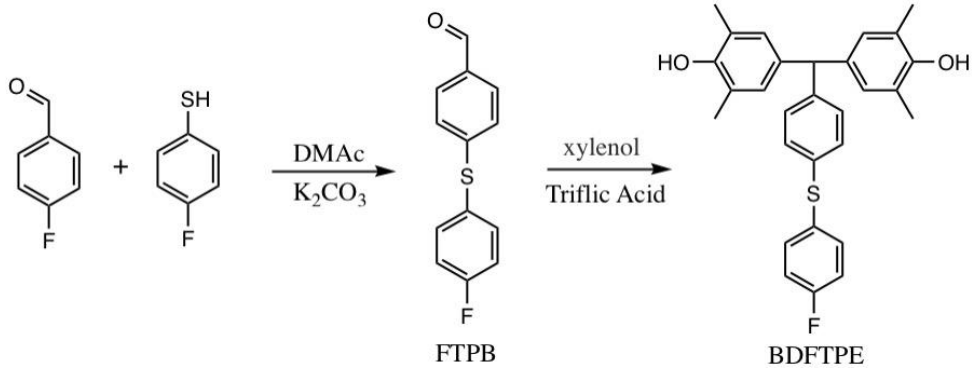

Fig. 1. Synthesis of the monomer

The NLO properties of the polymer mainly depend on the microstructure of molecular and measurement conditions. This report has systematically studied the nonlinear optical properties of OAESF and calculated the first and second hyperpolarizability on its static and frequency by DFT method.

This study aims to determine the size of oligomers and the effects of side chain substitution and absence on nonlinear optical properties. The results may provide valuable guidance for the design and synthesis of polymeric NLO materials.

2 EXPERIMENTAL

2. 1 Materials and measurements

4-Fluorobenzaldehyde(FBA), 4-fluorothiophenol (FBT) and 2,6-dimethylphenol were purchased from Shanghai Macklin Biochemical Technology Co, Ltd. Triflic acid, K_2CO_3 and 4,4′-difluorophenyl sulfone (DFPS) were commercial from TCI Co, Ltd. DMAc was available from Sinopharm Co, Ltd (Beijing, China) and redistilled before use. The ^{1}H NMR and ^{19}F spectra of monomer and oligomer were recorded on an AVANCE III at 400 MHz using deuterated dimethyl sulfoxide (DMSO-d_6) and chloroform-d as solvents. The mechanical agitator of precipitating monomer was purchased from Shanghai Yike Instrument Co, Ltd.

2. 2 Synthesis of monomer

The synthesis of 4-((4-fluorophenyl)thio)phenyl benzaldehyde (FTPB) K_2CO_3 (4.84 g, 35 mmol) was added to a solution of FBA (7 mL, 65 mmol) and FBT (7.45 mL, 70 mmol) in anhydrous DMAc (100 mL). The mixture with magnetic stirrer was then heated to 60 °C under nitrogen overnight and precipitated in 500 mL water. In the next step, the turbid mixture was extracted with 150 mL diethyl ether to get two homogeneous phases. The organic layer was concentrated with rotary evaporator to yield white oily solid. Yield: 93%. ^{1}H NMR(DMSO-d_6, ppm): 9.92(s, 1H), 7.81～7.83(d, J = 8.3Hz, 2H), 7.62～7.66(dd, J = 8.68Hz, 5.4Hz, 2H), 7.38(m, 2H), 7.27～7.28(d, J = 8.3Hz, 2H). ^{19}F NMR (DMSO-d_6, ppm): –111.27(s, 1F).

The synthesis of 1,1-bis(2,6-dimethylphenol)-1-(4-(4-fluorophenyl)thio)phenyl ethane (BDFTPE) FTPB (7 g, 30 mmol) and 2,6-dimethylphenol (11 g, 90 mmol) were added to a 100 mL round-bottomed flask under nitrogen atmosphere. Then the mixture was heated with magnetic stirrer to 50 °C until the solids are dissolved. Triflic acid (0.7 mL, 7.5 mmol) as catalyst was added to the dissolved solution rapidly and the temperature was increased to 60 °C

for 1.5 h. Distilled water (100 mL) was poured into the resulting violet viscous liquid, obtaining orange solid after violent mechanical stirring under 1200 rpm. The product was washed and filtrated to give a yellow solid. Yield: 82%. ^{1}H NMR (DMSO-d_6, ppm): 8.06(s, 2H), 7.37～7.41(m, 2H), 7.18～7.25(m, 4H), 7.04～7.06(d, J = 8.1Hz, 2H), 6.60(s, 4H), 5.20(s, 1H), 2.07(s, 12H). ^{19}F NMR (DMSO-d_6, ppm): –113.78(s, 1F).

2. 3 Synthesis of oligo(aromatic ether sulfone)-F

As shown in Fig. 2, BDFTPE (0.912 g, 2 mmol), DFPS (0.508 g, 2 mmol) and K_2CO_3 (0.69 g, 5 mmol) were added in 50 mL anhydrous DMAc and 10 mL toluene. A Dean-Stark trap was fitted on the 100 mL three-necked round-bottomed flask in which the mixture was put. The temperature was raised to 140 °C for 1 h. Then the system was heated to 147 °C to distill off water and toluene for about 10 min. The mixture was precipitated in a mixture of methanol and distilled water (30/30) after concentration. The product was collected by centrifugal sedimentation and filtration. A white powder can be obtained by washing and drying at 80 °C under vacuum. Yield: 71%. ^{1}H NMR ($CDCl_3$, ppm): 7.72～7.75(m, Ar), 7.32～7.36(m, Ar), 7.10～7.12(m, Ar), 6.93～6.98(m, Ar), 6.74～6.76(m, Ar), 5.29(s, 1H), 1.94(s, 12H). ^{19}F NMR ($CDCl_3$, ppm): –113.44(s, 1F).

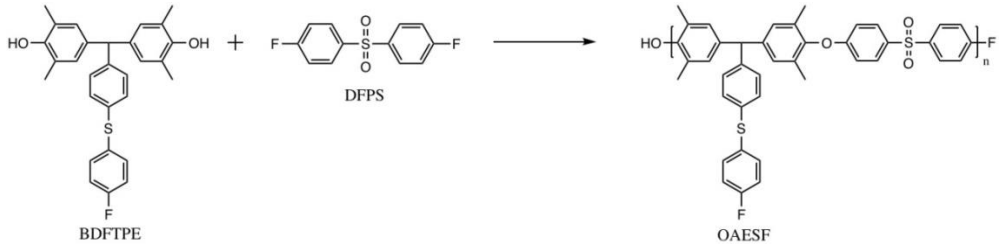

Fig. 2. Synthesis of OAESF

3 THEORY AND COMPUTATION

The *ab initio* calculation method based on density functional theory (DFT)[21] is an effective tool for predicting the electronic and optical properties of compounds. The ground state geometry of $OAESF_n$ is fully optimized based on B3LYP functional[22] and def2-sv (p) double-zeta basis sets[23], with D3 dispersion correction of Grimme[24]. The calculation of nonlinear hyperpolarizability is carried out in def2-svp basic sets with PBE0 hybrid functional[25]. With the double zeta basic sets, PBE0 functional may have better performance in valence excitation. All calculations were performed with the ORCA 4.2.1 program packages[26]. Multiwfn software was used to analyze the electronic structure, excitation characteristics and hyperpolarizability[27].

The sum-over-states (SOS) method is a common method of nonlinear optical calculation[28]. Static and frequency-dependent polarizabilities and hyperpolarizabilities can be calculated from the energy of each excited state and the transition dipole moment between each excited state. As shown in the following formula[28]:

$$\beta_{ABC}\left(-\omega_\sigma;\omega_1,\omega_2\right)=\hat{P}\left[A\left(-\omega_\sigma\right),B\left(\omega_1\right),C\left(\omega_2\right)\right]\sum_{i\neq 0}\sum_{j\neq 0}\frac{\mu_{0i}^{A}\overline{\mu_{ij}^{B}}\mu_{j0}^{C}}{\left(\Delta_i-\omega_\sigma\right)\left(\Delta_j-\omega_2\right)}$$

$$\gamma_{\mathrm{ABCD}}\left(-\omega_\sigma;\omega_1,\omega_2,\omega_3\right)=\hat{P}\left[A\left(-\omega_\sigma\right),B\left(\omega_1\right),C\left(\omega_2\right),D\left(\omega_3\right)\right]\left(\gamma^{\mathrm{I}}-\gamma^{\mathrm{II}}\right)$$

$$\gamma^{\mathrm{I}}=\sum_{i=0}\sum_{j=0}\sum_{k=0}\frac{\mu_{0i}^{A}\overline{\mu_{ij}^{B}}\mu_{jk}^{C}\mu_{k0}^{D}}{\left(\Delta_i-\omega_\sigma\right)\left(\Delta_j-\omega_2-\omega_3\right)\left(\Delta_k-\omega_3\right)}$$

$$\gamma^{\mathrm{I}}=\sum_{i\neq 0}\sum_{j=0}\frac{\mu_{0i}^{A}\mu_{i}^{B}\mu_{0j}^{C}\mu_{j0}^{D}}{\left(\Delta_i-\omega_\sigma\right)\left(\Delta_i-\omega_1\right)\left(\Delta_j-\omega_3\right)}$$

A, B, C... denote one of the directions {x, y, z}; ω is energy of external fields; Δ_i stands for the excitation energy of state i with respect to the ground state 0; μ_{ij}^{A} is A component of the transition dipole moment between states i and j.

The calculation of nonlinear optical susceptibility is to calculate the response of molecular wave function to external field. The Finite Field (FF) and Coupled Perturbed Hartree-Fock/Kohn-Sham (CPHF/KS) methods are based on the influence of external electric field on the static Schrodinger equation to calculate the higher-order derivative of energy to the external field. The Sum-Over-States (SOS) method is based on the time-dependent density functional theory to calculate the response of wave function to external field perturbation. The advantage of SOS method lies in its high efficiency in calculating frequency dependent nonlinear polarizability. When the number of States is enough, the SOS method is theoretically accurate.

The magnitude of hyperpolarizability is used to quantitatively study the nonlinear polarizability of the system[32]:

$$\beta_{\mathrm{tot}} = \sqrt{\beta_x^2 + \beta_y^2 + \beta_z^2}$$

$$\gamma_{\mathrm{tot}} = \sqrt{\gamma_x^2 + \gamma_y^2 + \gamma_z^2}$$

4 RESULTS AND DISCUSSION

4. 1 Study of oligomer constitutional unit

Aiming to study the nonlinear optical properties of $OAESF_n$, the unit spherical representation was utilized for probing the anisotropy of polarizability α of OAESF constitutional unit, as showed in Fig. 3. It illustrates that the constitutional unit has a large polarizability in the direction of backbone. A significant electricity-induced dipole moment indicates the anisotropy of the polarizability of the oligomer molecule. The optical response of OAESF system along the backbone is more prominent[29].

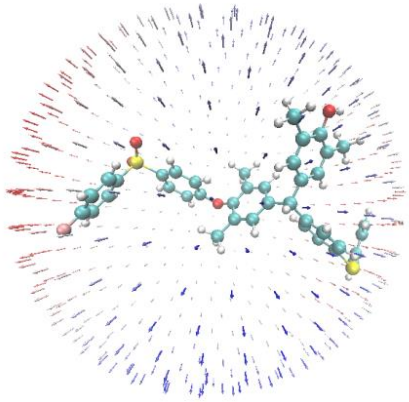

Fig. 3. Anisotropy of polarizability α of OAESF constitutional unit

In order to illustrate the accuracy of the calculated linear and nonlinear optical coefficients, CPHF method under CAM-B3LYP/6-31+G (d,p) and SOS method under PBE0/def2-SVP and SOS-ZINDO are compared. It can be seen that the calculation accuracy of Sum-Over-States method in this system can be guaranteed.

Table 1. Nonlinear Optical Coefficients of OAESF Calculated by Different Methods

	CPHF	SOS	
Linear and nonlinear optical coefficients (a.u.)	CAM-B3LYP/6-31+G (d,p)	PBE0/def2-SVP	ZINDO
α	160.43	139.56	150.76
γ	1.59322E+05	1.78056E+05	1.43504E+05

Then the second and third nonlinear optical polarizability density along the backbone was calculated. Contrast between the dipole moment after Taylor expansion and electron density gives hyperpolarizability of oligomer unit as follows[30].

$$\boldsymbol{\mu}(\mathbf{F}) = -\frac{\partial E}{\partial \mathbf{F}} = \boldsymbol{\mu}_0 + \boldsymbol{\alpha}\mathbf{F} + (1/2)\boldsymbol{\beta}\mathbf{F}^2 + (1/6)\gamma\mathbf{F}^3 + \ldots$$

$$\rho(\mathbf{r},\mathbf{F}) = \rho^{(0)}(\mathbf{r}) + \mathbf{p}^{(1)}(\mathbf{r})\mathbf{F} + (1/2)\mathbf{p}^{(2)}(\mathbf{r})\mathbf{F} + (1/6)\boldsymbol{\rho}^{(3)}(\mathbf{r})\mathbf{F}^3 + \ldots$$

$$\rho_{xx}^{(2)} = \frac{\rho\left(F^x\right) - 2\rho(0) + \rho\left(-F^x\right)}{\left(F^x\right)^2}$$

$$\beta_{xxx} = \int -\rho_{xx}^{(2)}(\mathbf{r}) x d\mathbf{r}$$

$$\gamma_{xxxx} = \int -\rho_{xxx}^{(3)}(\mathbf{r}) x d\mathbf{r}$$

$$\rho_{xxx}^{(3)} = \frac{\rho\left(2F^x\right) - 2\rho\left(F^x\right) + 2\rho\left(-F^x\right) - \rho\left(-2F^x\right)}{2\left(F^x\right)^3}$$

Using the above formula, the finite difference is performed with 0.003 a.u. as the step size, and the hyperpolarizability density of OAESF is obtained. The calculated hyperpolarizability density $\rho_x^{(n)}$ shown in Fig. 4 confirms that the polymer unit molecules provide a general contribution to the second-order nonlinear optical polarizability. It can be seen from the atomic space integral that both the main and side chains contribute to β. For γ, the contribution of the side chain is relatively high. Consequently, the increasing degree of polymerization tends to make a positive influence to the NLO polarizabilities.

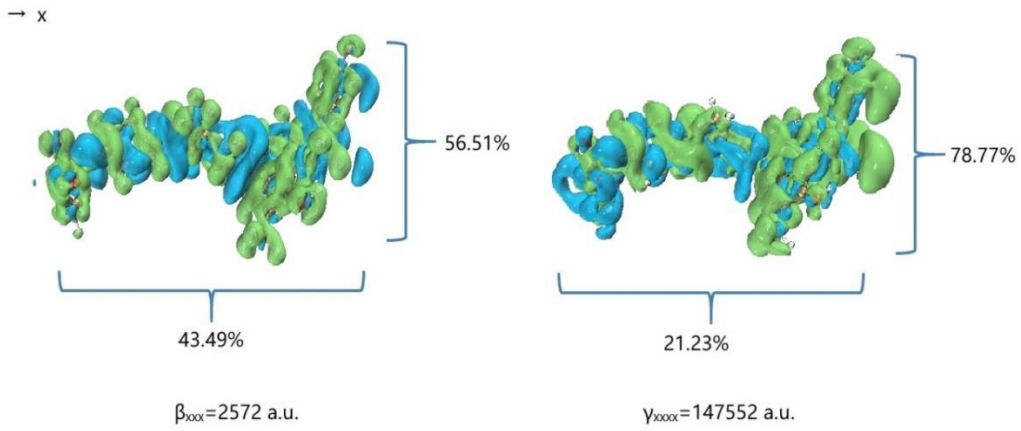

Fig. 4. The second-order (left) and third-order (right) nonlinear polarizability density of OAESF constitutional unit (Positive isosurfaces are shown in green)

4. 2 Effect of degree of oligomerization

Fig. 5 shows the relationship between the degree of oligomerization and its energy gap $\Delta E_{H\text{-}L}$. The rate of decreasing band gap is declining as the degree of oligomerization grows. The NLO properties can be approximated by TD-ZINDO-SOS method with results shown in Fig. 6. The alteration of nonlinear optical coefficient tends to be gentle with the expanding size of oligomer. Subsequent study was based on the modification of $OAESF_3$ for its highly typicality.

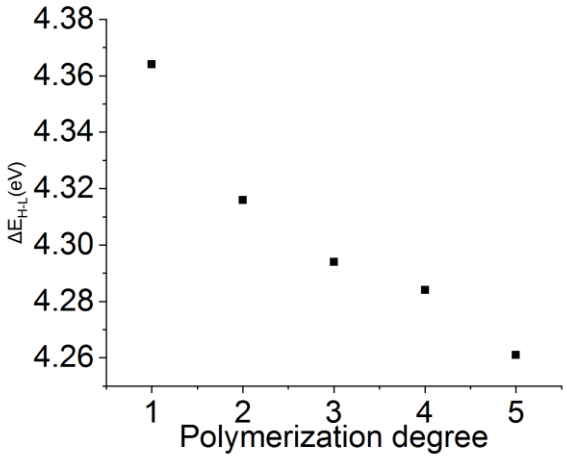

Fig. 5. Relationship between the $OAESF_n$ polymerization degree and HOMO-LOMO energy gap

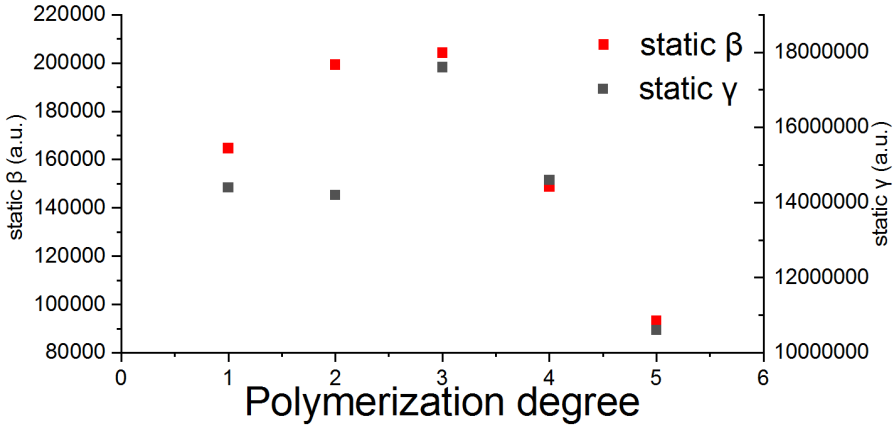

Fig. 6. Relationship between the $OAESF_n$ polymerization degree and the second order (β) and third order (γ) nonlinear polarizability

4. 3 Static and frequency-dependent NLO properties of $OAESF_3$ with side chain substituted and deleted

Table 2 shows the calculation of ΔE_{H-L} for different proportions of substituted phenyl or the absence of side chain. It may be noticed that the electronic structure of the polymer $OAESF_3$ changes with the structure of the side chain. The replacement of the side chain affects the HOMO and LUMO orbitals, which lead to the gradual reduction of ΔE_{H-L}, while the absence of side chain amplifies ΔE_{H-L}.

Table 2. ΔE_{H-L} (eV) for $OAESF_3$ with Different Proportions of Substituted Phenyl or the Absence of Side Chain

	0	33%	66%	100%
$OAESF_3$-sub	4.294	4.229	4.212	4.201
$OAESF_3$-abs	4.294	4.31	4.336	4.438

Table 3 lists the vertical excitation features calculated by TDDFT under the substitution and absence of side chains. It states that the electronic excitation properties of $OAESF_3$ depend not only on the HOMO and LOMO orbitals, but also on the contributions of other excited states. $OAESF_3$ may have some potential in the application of frequency doubling due to its absorption in deep ultraviolet region.

Table 3. Crucial Vertical Excitation Properties of $OAESF_3$ and Derivatives

Molecule	λ_{max}*	f*	Electronic transition
OAESF3	274.05	0.47758	H*-1 -> L*+10 67.1%, H-1 -> L+9 6.7%
OAESF3 sub 33%	299.71	0.79899	H -> L+3 89.3%
	274.03	0.43487	H-2 -> L+9 73.5%
OAESF3 sub 66%	298.9	1.06938	H -> L+4 79.9%, H-1 -> L+3 7.7%
	250.2	0.70977	H-7 -> L+2 28.6%, H-8 -> L+2 17.8%, H-6 -> L+2 13.2%
OAESF3 sub 100%	298.93	1.13298	H-1 -> L+4 76.0%, H-2 -> L+3 11.5%
	249.84	1.36583	H-8 -> L+1 27.8%, H-10 -> L 25.9%, H-7 -> L+1 22.4%
OAESF3 abs 33%	251.2	0.48126	H-11 -> L 23.1%, H-7 -> L 11.8%, H-1 -> L+17 10.4% , H-1 -> L+5 8.8%,
	274.13	0.4282	H-1 -> L+8 53.2%, H-1 -> L+7 23.1%
OAESF3 abs 66%	249.93	1.178	H-6 -> L 36.7%, H-5 -> L+1 25.4%, H-10 -> L+1 15.3%
OAESF3 abs 100%	251.38	0.68929	H-4 -> L+2 40.2%, H-3 -> L+2 38.1%, H-5 -> L 5.2%

* λ_{max} is the maximum absorption wavelength while f refers to the maximum of oscillation strength. H and L denote HOMO and LUMO, respectively

At the PBE0/def2-svp level, 100 excited states are calculated using TDDFT for the SOS method. The accuracy of SOS method largely depends on the convergence of the calculated results. Herein the convergence of the method was tested firstly. As shown in Fig. 7, 100 excited states can meet the requirements of computational precision and accuracy.

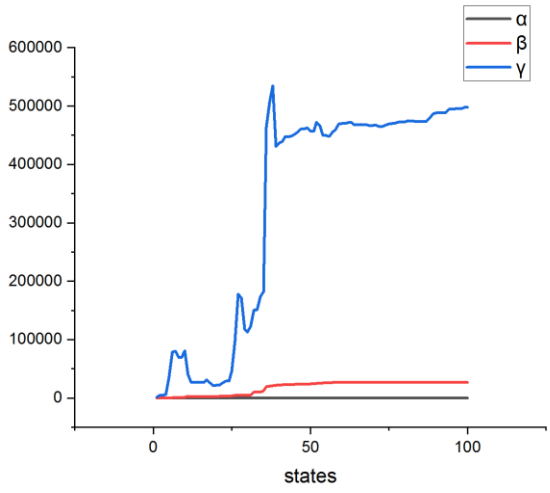

Fig. 7. Convergence of applying SOS method to $OAESF_3$

Then the static polarizabilities and the first and second hyperpolarizabilities of substituted and side chain deleted $OAESF_3$ were calculated, as shown in Table 2. What can be known is that the absence of side chain results in the reduction of ΔE_{H-L}, which accordingly reduces the nonlinear polarizability along the backbone. The substitution on side chains is increasing in general, but the excessive substitution can lower the hyperpolarizability, which may be caused by the enhancement of electronic delocalization in the direction of side chains owing to the overmuch substituent. It illustrates that the absence/substituted proportion plays a key role in regulating the nonlinear optical properties of OAESF materials. We can be see from the fitting of ΔE_{H-L} and static nonlinear optical coefficients that an approximate relative linearity exists respectively between static polarizability, hyperpolarizability and ΔE_{H-L}, as depicted in Fig. 8[31].

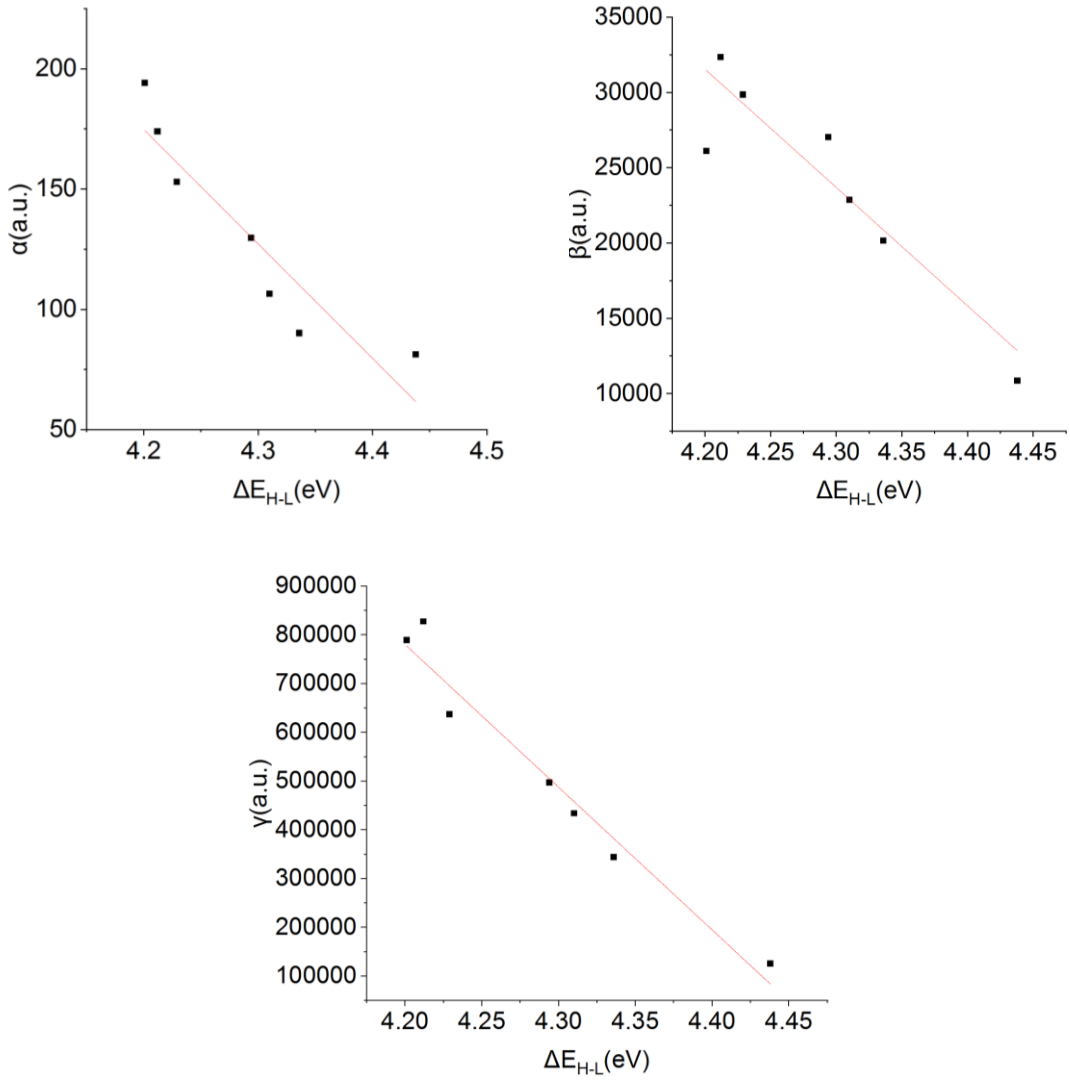

Fig. 8. Relationship between the electronic polarizability and hyperpolarizability with energy gap ΔE_{H-L} for $OAESF_3$ and derivatives

Subsequent calculation utilized SOS method to the nonlinear polarizability of the second harmonic generation, Kerr effect, electrically-induced second harmonic and third harmonic generation, and degenerated four wave mixing (DFWM) at the wavelength of 350～750 nm, as shown in Fig. 9. When the frequency of the incident light is equal to or close to the natural frequency of the harmonic oscillator in the medium, the abnormal dispersion will occur due to resonance. At this time, the value of nonlinear optical polarizability with frequency is very large, which has only qualitative significance. It can be noted that increasing the phenyl substituents of the side chain can significantly improve the static nonlinear polarizability and the frequency nonlinear polarizability. For OAESF system, the increase of side chain substitution can make the third-order nonlinear optical absorption peak red shift. However, the loss of side chain will cause the third-order nonlinear optical absorption peak to slightly blue shift. It is possible to change the nonlinear optical properties of the whole oligomer through side chain chemical regulation. These properties can be applied to optically modulate the OAESF polymer materials. The $OAESF_s$-based polarized membrane materials may have promising applications in fields like adjustable electro-optic switching and fiber optic sensing.

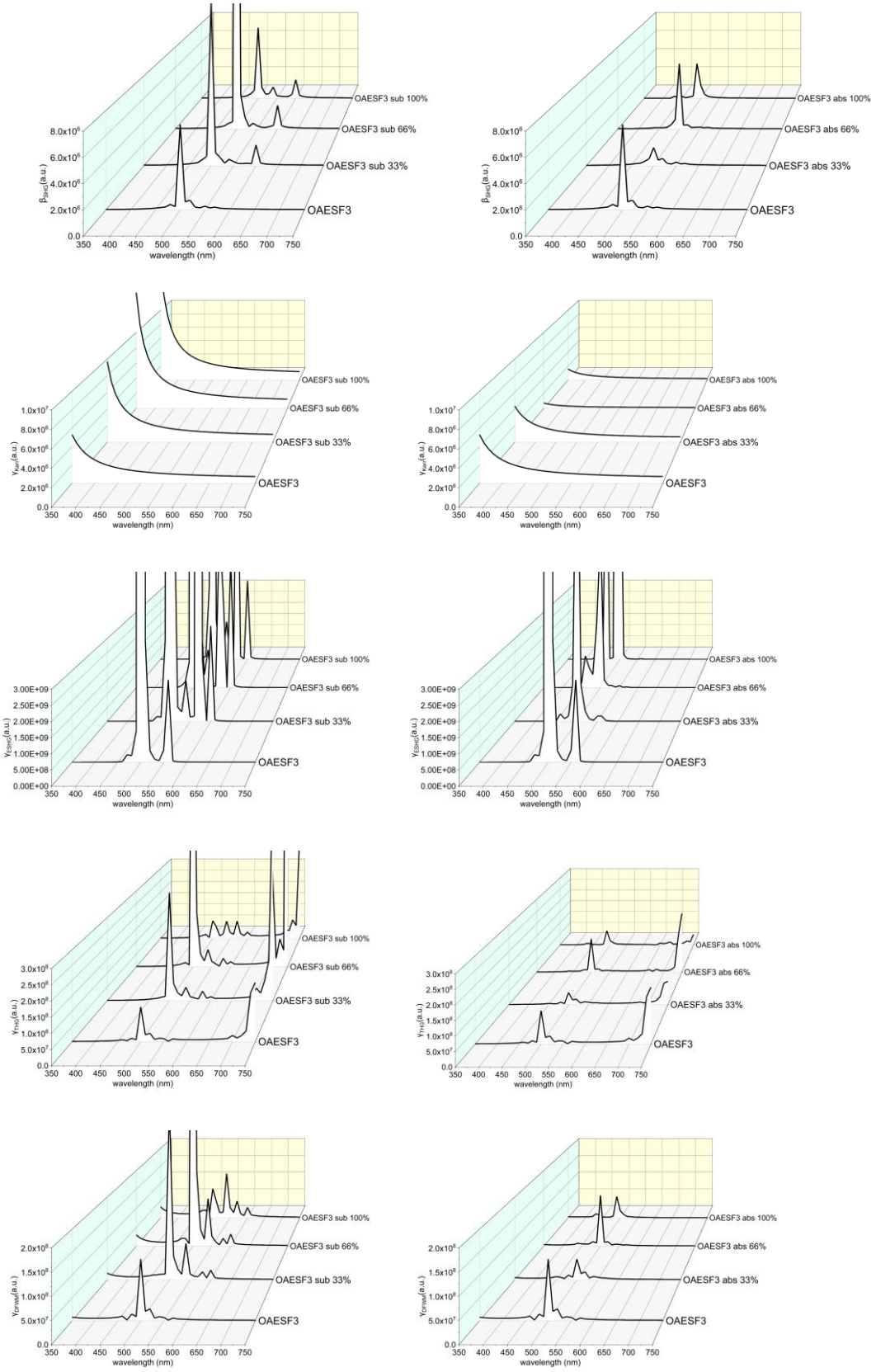

Fig. 9. Frequency-dependent NLO coefficients of $OAESF_3$ and derivatives

5 CONCLUSION

In this work, a novel oligomer of PAESF was synthesized and characterized. The electronic structure of OAESF was studied by DFT method. The effects of side chain absence and substitution on the linear optical coefficients and the second- and third-order nonlinear optical coefficients of OAESF were studied on the basis of $OAESF_3$. The loss of side chain will reduce ΔE_{H-L}, and then the nonlinear optical polarizability of the polymer. A reasonable range of substitution can improve ΔE_{H-L} and the overall nonlinear polarizability of oligomers. At the same time, the loss and substitution of side chains can lead to the red/blue shift of nonlinear polarizability. The nonlinear optical properties of the oligomer can be adjusted by regulating the molecular structure and incident light frequency. This study provides a reference for the design and synthesis of nonlinear polarized membrane optical devices.

REFERENCES

(1) Moliton, A.; Hiorns, R. C. Review of electronic and optical properties of semiconducting π-conjugated polymers: applications in optoelectronics. *Polym. Int.* **2004**, 53, 1397–1412.

(2) Burland, D. M.; Miller, R. D.; Walsh, C. A. Second-order nonlinearity in poled-polymer systems. *Chem. Rev.* **1994**, 94, 31–75.

(3) Champagne, B.; Kirtman, B. Theoretical approach to the design of organic molecular and polymeric nonlinear optical materials. *Handbook of Advanced Electronic and Photonic Materials and Devices*. Academic Press **2001**, 63–126.

(4) Cho, M. J.; Choi, D. H.; Sullivan, P. A.; Akelaitis, A. J. P.; Dalton, L. R. Recent progress in second-order nonlinear optical polymers and dendrimers. *Prog. Polym. Sci.* **2008**, 33, 1013–1058.

(5) Heeger, A. J. Semiconducting and metallic polymers: the fourth generation of polymeric materials (Nobel lecture). *Angew. Chem. Int. Ed.* **2001**, 40, 2591–2611.

(6) Liyanage, P. S.; de Silva, R. M.; de Silva, K. M. N. Nonlinear optical (NLO) properties of novel organometallic complexes: high accuracy density functional theory (DFT) calculations. *J. Mol. Struc-Theochem.* **2003**, 639, 195–201.

(7) Maury, O.; Le Bozec, H. Molecular engineering of octupolar NLO molecules and materials based on bipyridyl metal complexes. *Accounts Chem. Res.* **2005**, 38, 691–704.

(8) Mehmood, U.; Al-Ahmed, A.; Hussein, I. A. Review on recent advances in polythiophene based photovoltaic devices. *Renew. Sust. Energ. Rev.* **2016**, 57, 550–561.

(9) Sun, H. T.; Jochen, A. Electronic energy gaps for π-conjugated oligomers and polymers calculated with density functional theory. *J. Chem. Theory Comput.* **2014**, 10, 1035–1047.

(10) Oviedo, M. B.; Ilawe, N. V.; Wong, B. M. Polarizabilities of π-conjugated chains revisited: improved results from broken-symmetry range-separated DFT and new CCSD (T) benchmarks. *J. Chem. Theory Comput.* **2016**, 12, 3593–3602.

(11) Zajac, M.; Hrobarik, P.; Magdolen, P.; Foltinova, P.; Zahradnik, P. Donor-π-acceptor benzothiazole-derived dyes with an extended heteroaryl-containing conjugated system: synthesis, DFT study and antimicrobial activity. *Tetrahedron* **2008**, 64, 10605–10618.

(12) Janjua, M. R. S. A.; Khan, M. U.; Bashir, B.; Iqbal, M. A.; Song, Y. Z.; Naqvi, S. A. R.; Khan, Z. A. Effect of π-conjugation spacer (CC) on the first hyperpolarizabilities of polymeric chain containing polyoxometalate cluster as a side-chain pendant: a DFT study. *Comput. Theor. Chem.* **2012**, 994, 34–40.

(13) Medved, M.; Budzak, S.; Pluta, T. Static NLO responses of fluorinated polyacetylene chains evaluated with long-range corrected density functionals. *Chem. Phys. Lett.* **2011**, 515, 78–84.

(14) Ogawa, K.; Zhang, T. Q.; Yoshihara, K.; Kobuke, Y. Large third-order optical nonlinearity of self-assembled porphyrin oligomers. *J. Am. Chem. Soc.* **2002**, 124, 22–23.

(15) Papadopoulos, M. G.; Sadlej, A. J.; Leszczynski, J. *Non-linear Optical Properties of Matter*. Dordrecht: Springer **2006**.

(16) Zhu, X.; Zheng, W. R.; Tang, X. F.; Zhang, W. B. Experimental and theoretical investigations of thermal degradation behaviors of poly(aryl ether sulfone)s. *J. Sulfur Chem.* **2018**, 39, 64–75.

(17) Zuo, P. Y.; Tcharkhtchi, A.; Shirinbayan, M.; Fitoussi, J.; Bakir, F. Overall investigation of poly(phenylene sulfide) from synthesis and process to applications—a review. *Macromol. Mater. Eng.* **2019**, 304, 1800686.

(18) Lade, H.; Kumar, V.; Arthanareeswaran, G.; Ismail, A. F. Sulfonated poly(arylene ether sulfone) nanocomposite electrolyte membrane for fuel cell applications: a review. *Int. J. Hydrogen Energ.* **2017**, 42, 1063–1074.

(19) Van der Bruggen, B. Chemical modification of polyethersulfone nanofiltration membranes: a review. *J. Appl. Polym. Sci*. **2009**, 114, 630–642.

(20) Li, Z.; Ding, J. F.; Robertson, G. P.; Guiver, M. D. A novel bisphenol monomer with grafting capability and the resulting poly(arylene ether sulfone)s. *Macromolecules* **2006**, 39, 6990–6996.

(21) Parr, R. G. Density functional theory of atoms and molecules. *Horizons of Quantum Chemistry*. Springer, Dordrecht **1980**, 5–15.

(22) Stephens, P. J.; Devlin, F. J.; Chabalowski, C. F.; Frisch, M. J. *Ab initio* calculation of vibrational absorption and circular dichroism spectra using density functional force fields. *J. Phys. Chem.* **1994**, 98, 11623–11627.

(23) Weigend, F.; Ahlrichs, R. Balanced basis sets of split valence, triple zeta valence and quadruple zeta valence quality for H to Rn: design and assessment of accuracy. *Phys. Chem. Chem. Phys.* **2005**, 7, 3297–3305.

(24) Adamo, C.; Barone, V. Toward reliable density functional methods without adjustable parameters: the PBE0 model. *J. Chem. Phys.* **1999**, 6158–6170.

(25) Grimme, S.; Antony, J.; Ehrlich, S.; Krieg, H. A consistent and accurate *ab initio* parametrization of density functional dispersion correction (DFT-D) for the 94 elements H-Pu. *J. Chem. Phys*. **2010**, 132, 154104.

(26) Neese, F. The ORCA program system. *WIRES Comput. Mol. Sci.* **2012**, 2, 73–78.

(27) Lu, T.; Chen, F. Multiwfn: a multifunctional wavefunction analyzer. *J. Comput. Chem.* **2012**, 33, 580–592.

(28) Meyers, F.; Marder, S. R.; Pierce, B. M.; Bredas, J. L. Electric field modulated nonlinear optical properties of donor-acceptor polyenes: sum-over-states investigation of the relationship between molecular polarizabilities (alpha, beta, and gamma) and bond length alternation. *J. Am. Chem. Soc*. **1994**, 116, 10703–10714.

(29) Tuer, A.; Krouglov, S.; Cisek, R.; Tokarz, D.; Barzda, V. Three-dimensional visualization of the first hyperpolarizability tensor. *J. Comput. Chem.* **2011**, 32, 1128–1134.

(30) Nakano, M.; Fukui, H.; Minami, T.; Yoneda, K.; Shigeta, Y.; Kishi, R.; Champagne, B.; Botek, E.; Kubo, T.; Ohta, K.; Kamada, K. (Hyper) polarizability density analysis for open-shell molecular systems based on natural orbitals and occupation numbers. *Theor. Chem. Acc.* **2011**, 130, 711–724.

(31) Li, H. P.; Bi, Z. T.; Xu, R. F.; Han, K.; Li, M. X.; Shen, X. P.; Wu, Y. X. Theoretical study on electronic polarizability and second hyperpolarizability of hexagonal graphene quantum dots: effects of size, substituent, and frequency. *Carbon* **2017**, 122, 756–760.

(32) Millefiori, S.; Alparone, A. *Ab initio* study of the molecular structure, polarizability and first hyperpolarizability of 6-hydroxy-1-formylfulvene. *J. Chem. Soc. Faraday T.* **1994**, 90, 2873–2879.